

## 本征点缺陷对硅材料响应特性的影响分析

吕彤, 张蓉竹\*

四川大学电子信息学院, 四川 成都 610065

**摘要** 针对硅基材料在 1319 nm 激光辐照下产生带外响应的问题,研究了硅材料中的本征点缺陷对响应特性的影响。根据第一性原理建立了晶胞模型,比较了几种典型点缺陷状态下硅材料的能级分布特性,在此基础上分析了本征点缺陷对硅材料光电响应特性的影响。结果表明:空位和自间隙原子两类缺陷都能够改变硅材料的能带结构和响应特性。532 nm 激光辐照时,硅基光敏单元的输出饱和阈值明显降低。当辐照波长为 1319 nm 时,硅材料产生明显的带外响应,其中贡献最大的是四面体间隙缺陷。此时材料带隙消失,吸收系数高达  $50391 \text{ cm}^{-1}$ ,折射率减小约 25.99%,因此硅材料在 1319 nm 处的量子效率值最大,导致光电响应最为强烈,输出饱和阈值最小,为  $0.0015 \text{ W} \cdot \text{cm}^{-2}$ 。

**关键词** 材料; 单晶硅; 光电响应; 本征点缺陷; 第一性原理

中图分类号 O436 文献标志码 A

DOI: 10.3788/AOS230916

## 1 引言

硅作为一种重要的半导体材料,因具有良好的光电响应特性在光电技术领域得到了广泛的应用<sup>[1-3]</sup>,人们针对硅基探测器的吸收响应特性展开了许多研究<sup>[4-5]</sup>。理论上,硅材料的响应长波极限约为 1100 nm,但是在实验中发现,硅器件在 1319 nm 的带外激光辐照下也会产生响应输出。2003 年,张大勇等<sup>[6]</sup>发现 1319 nm 激光能对可见光 CCD 造成干扰,并测到实现饱和和串扰、全屏饱和的激光功率密度阈值。2008 年,张磊<sup>[7]</sup>采用 1319 nm 及其组合激光辐照硅,发现硅对 1319 nm 激光有随辐照功率增大而饱和的现象,波段内激光的加入增强了硅对波段外激光的吸收。2011 年,邱冬冬等<sup>[8]</sup>研究发现硅材料对 1319 nm 的激光也有响应,并且认为这种带外响应是由本征吸收以外的其他吸收机制导致的。越来越多的实验观测结果表明硅基材料的光电响应特性偏离了理论情况,这对高精度探测产生了很明显的干扰。硅材料出现带外响应,说明其能带结构发生了变化。

硅中两种本征点缺陷分别是空位和自间隙原子,它们是晶体中固有的、不可消除的热点缺陷。空位和自间隙原子都会在硅中引入额外的电子态和空穴态,改变原有的带隙,从而影响材料的质量和器件的性能,因此人们针对本征点缺陷在硅中的行为进行了许多研究<sup>[9-11]</sup>。2000 年,Pei 等<sup>[12]</sup>研究发现在各类空位缺陷中单空位体系的形成能最低,空位缺陷以及六边形间隙缺陷均在材料带隙内出现局域态密度的峰值,而四面

体间隙缺陷的态密度实际上位于导带和价带区域。2007 年,Dannefaer 等<sup>[13]</sup>研究发现高温退火将导致硅中的单空位浓度明显降低,双空位浓度增加。2011 年, Lee 等<sup>[14]</sup>研究发现单晶硅的电导率与空位浓度呈幂律反比关系。2012 年,卜琼琼等<sup>[15]</sup>研究发现缺陷导致禁带宽度改变,硅的光响应范围增大,相同浓度下空位缺陷对带隙的影响较小。2019 年,毛亦尘等<sup>[16]</sup>研究发现硅晶体的热导率随两种点缺陷浓度的增加而逐渐减小,且受间隙原子的影响更大。

现有关于本征点缺陷的工作大多是针对缺陷性质及其对材料特性影响的研究,而进一步对于硅材料的光电响应特性存在的干扰并没有直接明确的研究报道。本文主要考虑空位和自间隙原子两种本征点缺陷对硅能级分布的影响,根据第一性原理和光电响应理论模型,对比分析各类缺陷对硅材料的能带结构及 1319 nm 激光辐照下的响应特性的影响。

## 2 本征点缺陷对能带结构的影响

研究硅中的两种本征点缺陷,需要从微观点阵结构出发,由于数据量很大,目前的计算模型只能覆盖缺陷周围的数个单元结构,无法对宏观上的整个硅基材料进行计算。本文的分析目标是对不同缺陷状态的影响进行对比,因此重点关注的是本征点缺陷引起材料性质的相对变化。考虑到晶体结构和缺陷浓度,主要研究肖特基、双空位、弗兰克尔、四面体间隙、六边形间隙以及双间隙原子几种缺陷类型对硅材料的影响。

收稿日期: 2023-05-04; 修回日期: 2023-05-31; 录用日期: 2023-06-08; 网络首发日期: 2023-06-28

通信作者: \*zhang\_rz@scu.edu.cn

## 2.1 含本征点缺陷的晶胞模型建立

硅的晶体结构为金刚石结构,其空间群为  $Fd\bar{3}m$ , 常温下的晶格常数约为 0.357 nm。根据硅的晶体特征,建立了含有 96 个原子的  $2 \times 2 \times 3$  硅超胞,分别采用

不同类型的空位和不同位置的自间隙原子来构建缺陷模型。含本征点缺陷的硅晶胞模型如图 1 所示,其中黄色的为硅原子,灰色的表示空位,红色的为自间隙原子。

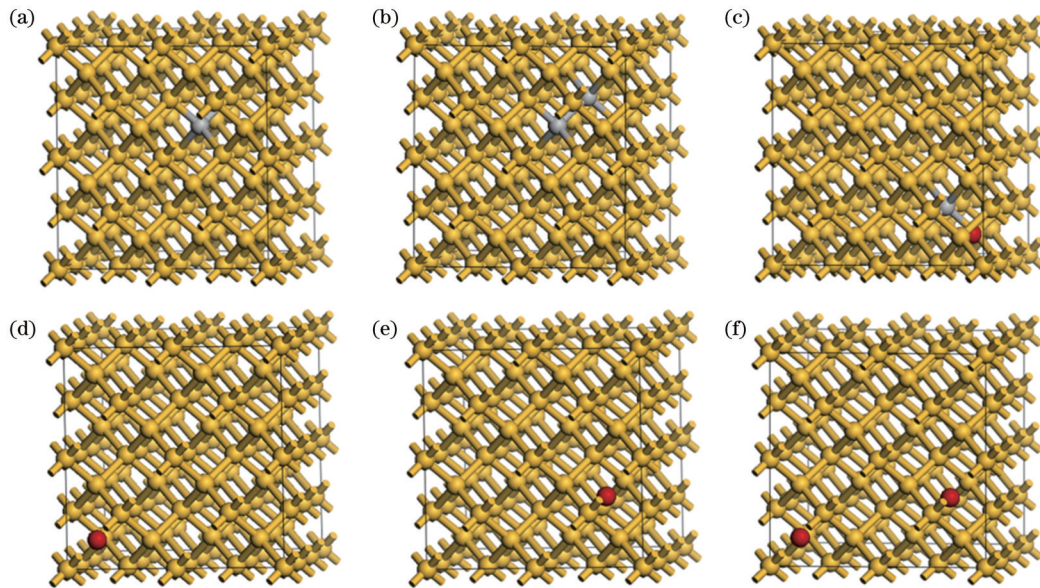


图 1 含本征点缺陷的硅晶胞模型。(a)肖特基缺陷;(b)双空位缺陷;(c)弗兰克尔缺陷;(d)四面体间隙缺陷;(e)六边形间隙缺陷;(f)双间隙原子缺陷

Fig. 1 Silicon cell models with intrinsic point defects. (a) Schottky defect; (b) divacancies defect; (c) Frankel defect; (d) tetrahedral interstitial defect; (e) hexagonal interstitial defect; (f) double-interstitial atomic defect

晶胞模型构建完成后,首先需要对体系进行几何结构优化。基于第一性原理,采用 Materials Studio 材料计算软件中的 CASTEP<sup>[17]</sup> (Cambridge Sequential Total Energy Package) 模块对两种本征点缺陷影响下的硅晶胞进行优化和计算,交换关联势相互作用通过广义梯度近似(GGA)中的 PBE<sup>[18]</sup> (Periodic Boundary Embedding) 泛函来描述。计算过程中采用超软赝势<sup>[19]</sup> (USP) 来描述离子实与价电子的相互作用,平面波截断能设置为 480 eV,布里渊区中 k 点网格设为  $2 \times 2 \times 2$ 。为了确保体系能量能够精确收敛,自洽场的收敛精度设为  $1.0 \times 10^{-6}$  eV/atom,原子间最大相互作用力、原子最大位移以及晶体最大内应力分别设为 0.003 eV/nm、0.0001 nm 和 0.05 GPa。

## 2.2 缺陷影响下硅材料的性质变化

当硅中不存在缺陷时,计算得到的材料带隙为 0.576 eV,比实际本征硅的带隙小,这是因为计算软件的交换关联泛函低估了材料的带隙值。空位和自间隙原子两种本征点缺陷都会在硅的禁带中引入缺陷能级,使得材料带隙减小甚至消失,这也是硅材料产生带外响应的重要原因。空位缺陷中,肖特基缺陷使得材料带隙消失,而双空位缺陷和弗兰克尔缺陷使得带隙分别减小为 0.087 eV 和 0.107 eV。对于自间隙原子缺陷,四面体间隙缺陷使得带隙消失,而六边形间隙缺陷和双间隙原子缺陷使得材料带隙分别减小为

0.464 eV 和 0.447 eV。

图 2 为本征硅及两种本征点缺陷影响下硅材料的态密度图(取费米能级为能量零点)。由图 2 可知,空位和自间隙硅原子都使得费米能级附近的态密度值明显增大,表明该能量附近的能级数量明显增多。同时硅材料的态密度整体向低能方向移动,这是因为本征点缺陷引入的额外能级与硅材料原有能带相互作用,使得能级重新分布,导致系统总能量降低。图 2(a)显示,本征硅在费米能级附近的态密度极小值(0.44816)位于 0.48216 eV 处。图 2(b)、(c)显示,当硅中分别存在肖特基缺陷和双空位缺陷时,态密度分别在 0.3159 eV 和 0.1555 eV 处出现新的态密度峰,表明该能量附近的能带变宽。图 2(d)显示,当硅中存在弗兰克尔缺陷时,态密度极小值(7.9040)位于 0.4893 eV 处。图 2(e)显示,四面体间隙缺陷使得硅材料在费米能级附近的极小值(0.6737)向左移动到 -0.5136 eV。图 2(f)显示,六边形间隙缺陷使得极小值(2.3187)向左移动到 0.2622 eV,且在 -0.3499 eV 处出现一个新的态密度峰。图 2(g)表明,当硅中存在双间隙原子缺陷时,态密度极小值(1.6175)位于 0.3081 eV 处。

空位和自间隙硅原子的存在均会改变硅材料的能带结构,因此也相应地改变材料的光学性质。图 3 所示为两种本征点缺陷影响下硅材料的吸收谱线,可以看出,空位缺陷和自间隙原子缺陷都会增强硅材料在

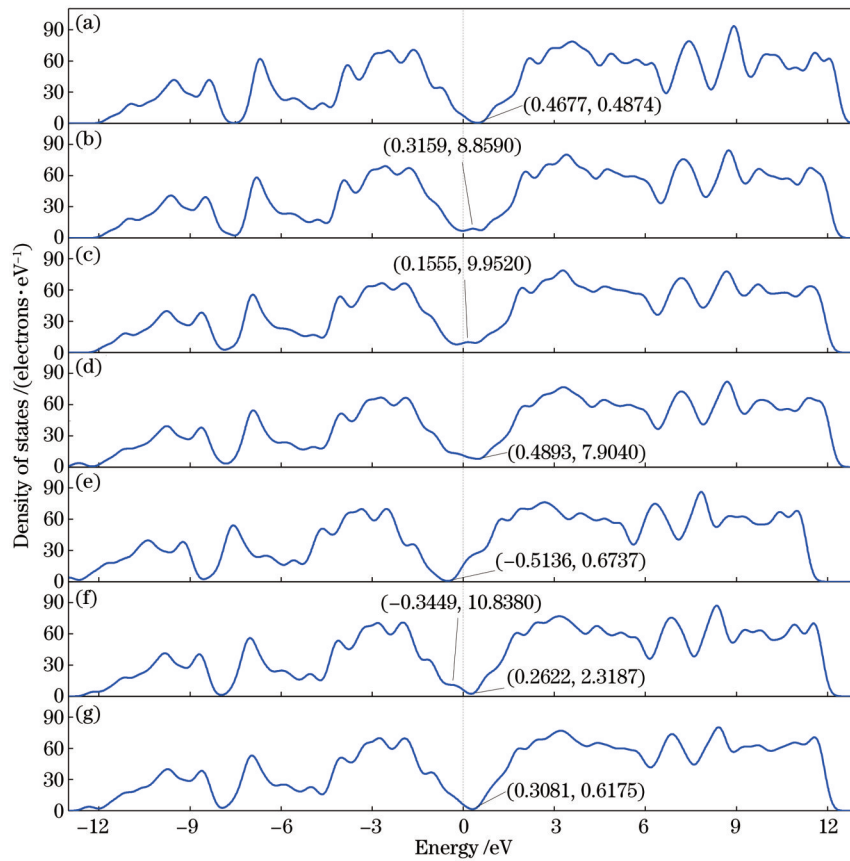


图 2 本征点缺陷影响下硅材料的态密度。(a)本征硅;(b)肖特基缺陷;(c)双空位缺陷;(d)弗兰克尔缺陷;(e)四面体间隙缺陷;(f)六边形间隙缺陷;(g)双间隙原子缺陷

Fig. 2 Density of states of silicon materials affected by intrinsic point defects. (a) Intrinsic silicon; (b) Schottky defect; (c) divacancies defect; (d) Frankel defect; (e) tetrahedral interstitial defect; (f) hexagonal interstitial defect; (g) double-interstitial atomic defect

可见光和红外波段的吸收,并使吸收极限向长波方向移动。在响应带外的光谱范围(波长大于 1100 nm),图 3(a)显示材料吸收系数在双空位缺陷影响下的变化相对明显,图 3(b)显示四面体间隙缺陷对吸收系数的影响相对明显,在本征硅理论上不产生响应的 1475 nm 处出现新的吸收峰,峰值约为  $51427\text{ cm}^{-1}$ 。相

同浓度的空位与自间隙缺陷相比,四面体间隙缺陷对于硅材料的吸收系数影响最大。此时,硅材料对 1319 nm 激光的吸收系数高达  $50391\text{ cm}^{-1}$ ,这就意味着硅材料能够对该波长下的带外光子产生强吸收,从而产生额外的响应输出。

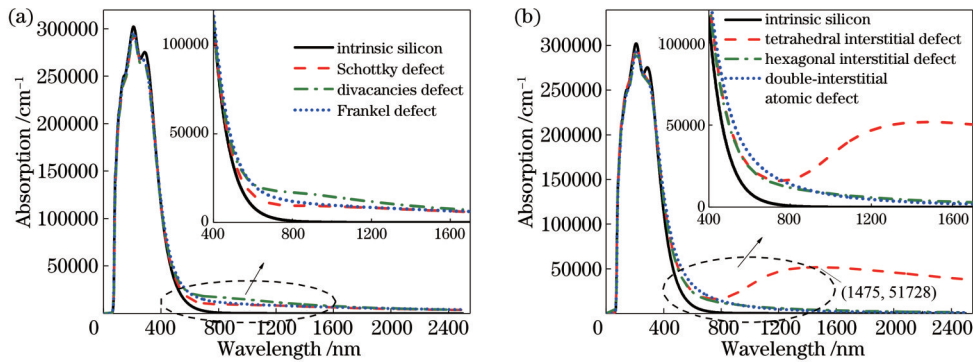


图 3 本征点缺陷影响下硅材料的吸收系数。(a)空位缺陷;(b)自间隙原子缺陷

Fig. 3 Absorption of silicon materials under the influence of intrinsic point defects. (a) Vacancy defects; (b) self-interstitial atomic defects

图 4 所示为本征点缺陷影响下硅材料的折射率曲线。可以看出,空位缺陷改变了可见光和红外波段内

硅材料的折射率变化趋势,使其随着波长的增大而呈现先减小后缓慢增大的趋势。在响应带外的波段范

围,空位缺陷、六边形间隙缺陷和双间隙原子缺陷影响下的折射率均大于本征状态。图 4(a)显示材料折射率在双空位缺陷影响下的变化相对明显,图 4(b)显示四面体间隙缺陷对折射率的影响相对明显,在

1060 nm 处出现极小值 2.363,此后折射率随波长持续增大。在相同缺陷浓度的情况下,四面体间隙缺陷使得材料折射率的变化最大,在 1319 nm 波长下的折射率相比于本征状态减小了 25.99%。

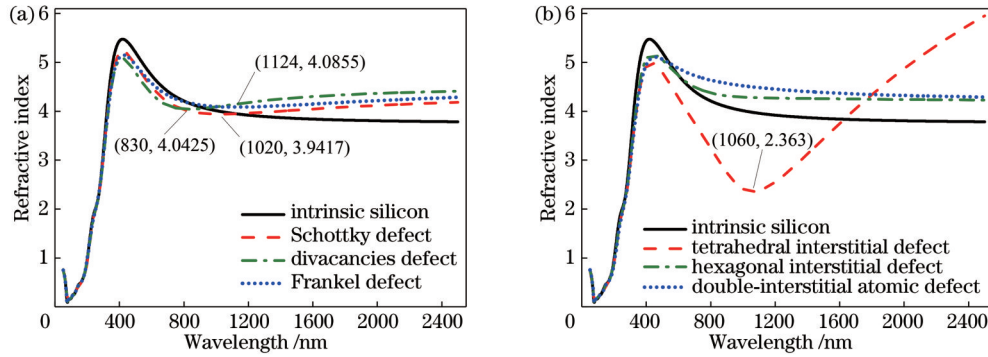


图 4 本征点缺陷影响下硅材料的折射率。(a)空位缺陷;(b)自间隙原子缺陷

Fig. 4 Refractive index of silicon materials under the influence of intrinsic point defects. (a) Vacancy defects; (b) self-interstitial atomic defects

### 3 硅材料的光电响应特性分析

理论上本征硅的响应极限约为 1100 nm,但从前文分析可知,空位和自间隙原子两种本征点缺陷的存在会使硅材料的能带结构和响应带外的光学性质发生

明显改变,这将导致额外的光电响应输出,也就是硅材料的带外响应现象。分别选取 532 nm 和 1319 nm 激光来比较不同类型缺陷对硅材料带内、带外响应特性的影响。计算所得的吸收系数  $\alpha$  和折射率  $n$  分别如表 1 和表 2 所示。

表 1 本征点缺陷影响下硅材料的吸收系数  $\alpha$

Table 1 Absorption  $\alpha$  of silicon materials affected by intrinsic point defects

Wavelength /nm	$\alpha / \text{cm}^{-1}$						
	Intrinsic silicon	Schottky defect	Divacancies defect	Frankel defect	Tetrahedral interstitial defect	Hexagonal interstitial defect	Double- interstitial atomic defect
532	21433	26776	31234	33312	39144	38309	48227
1319	10.998	7619.7	10256	7790.2	50391	4835.6	3607.8

表 2 本征点缺陷影响下硅材料的折射率  $n$

Table 2 Refractive index  $n$  of silicon materials affected by intrinsic point defects

Wavelength /nm	Refractive index $n$						
	Intrinsic silicon	Schottky defect	Divacancies defect	Frankel defect	Tetrahedral interstitial defect	Hexagonal interstitial defect	Double- interstitial atomic defect
532	5.0411	4.7961	4.6380	4.8168	4.6334	4.9448	5.0052
1319	3.8878	3.9852	4.2240	4.1014	2.8774	4.2642	4.4214

#### 3.1 缺陷影响下的量子效率

量子效率是半导体光电探测器的重要指标,量子效率越高,表明光电器件对入射光的转换效率越高,器件具有更好的光电性能。基于在器件表面由反射作用以及光线穿过一定厚度的接触层所造成的光子损耗,定义量子效率<sup>[20]</sup>  $\eta$  为

$$\eta = (1 - R_i) \cdot \exp(-\alpha \cdot h) \cdot [1 - \exp(-\alpha \cdot H)], \quad (1)$$

式中: $h$ 为前端接触层厚度; $H$ 为吸收层厚度; $R_i$ 为表面反射率; $\alpha$ 为吸收系数。反射率  $R_i$  与折射率  $n$  及吸收系

数  $\alpha$  的关系为

$$R_i = \frac{(1 - n)^2 + \left(\frac{\lambda\alpha}{4\pi}\right)^2}{(1 + n)^2 + \left(\frac{\lambda\alpha}{4\pi}\right)^2}. \quad (2)$$

根据表 1 和表 2 所列参数及式(1),可计算得到两类本征点缺陷影响下硅材料的量子效率,如图 5 所示。可以看出,本征点缺陷影响下硅材料的量子效率与其吸收系数具有类似的变化规律,这是因为量子效率与

材料吸收系数密切相关,吸收系数越大,量子效率也相应变大。图 5(a)显示双空位缺陷对量子效率的增强效果相对明显,图 5(b)显示四面体间隙缺陷对于硅材料量子效率的影响相对明显,在理论上不发生响应的 1255 nm 处出现峰值 0.29237。当这几种缺陷浓度相

同时,四面体间隙缺陷使得硅材料在红外波段的量子效率值最大,1319 nm 处对应的量子效率为 0.2901,因此硅材料在该波长下能够产生明显的带外响应输出现象。当 532 nm 和 1319 nm 激光辐照时,各类缺陷影响下硅材料的量子效率如表 3 所示。

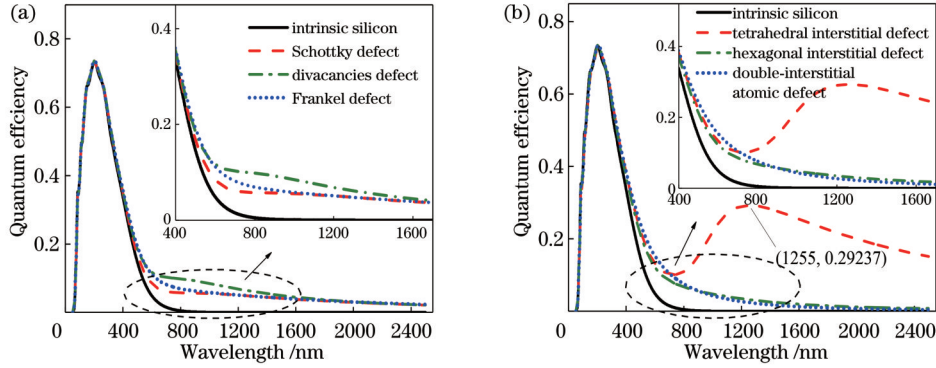


图 5 本征点缺陷影响下硅材料的量子效率。(a)空位缺陷;(b)自间隙原子缺陷

Fig. 5 Quantum efficiency of silicon materials affected by intrinsic point defects. (a) Vacancy defects; (b) self-interstitial atomic defects

表 3 本征点缺陷影响下硅材料的量子效率  $\eta$

Table 3 Quantum efficiency  $\eta$  of silicon materials affected by intrinsic point defects

Wavelength /nm	Quantum efficiency $\eta$						
	Intrinsic silicon	Schottky defect	Divacancies defect	Frankel defect	Tetrahedral interstitial defect	Hexagonal interstitial defect	Double-interstitial atomic defect
532	0.10543	0.13231	0.15406	0.15857	0.18534	0.17461	0.20712
1319	$7.16 \times 10^{-5}$	0.04687	0.06002	0.04705	0.29010	0.02898	0.02128

### 3.2 硅材料的光电响应特性

对于正常工作的硅基光敏单元,光电转换产生的信号电量<sup>[21]</sup>可以表示为

$$\int_0^{Q_s} \frac{dQ_s}{1 - \exp(-\alpha x_d)} = eSg_0 I_0 t, \quad (3)$$

式中: $Q_s$ 为信号电量; $\alpha$ 为光吸收系数; $x_d$ 为耗尽层深度; $e$ 为电子电量; $S$ 为耗尽层面积; $I_0$ 为入射光辐照功率密度; $t$ 为采样时间; $g_0 = \eta(1 - R_f)/(h\nu)$ ,其中 $\eta$ 为量子效率, $R_f$ 为表面反射率, $\nu$ 为入射光频率。

根据硅基探测器的相关典型参数<sup>[22]</sup>,信号电量达到  $6.76 \times 10^{-13}$  C 时可将硅基光敏单元视为饱和,这也对应了硅材料光电转换的极限。图 6 所示为 532 nm 激光辐照下本征点缺陷对硅材料响应特性的影响。可以看出,当辐照光波长为 532 nm 时,缺陷也会增强硅材料在可见光波段内的响应输出,导致硅基光敏单元的输出饱和阈值在不同本征点缺陷的影响下分别有不同程度的降低。图 6(a)显示,按不同类型的空位缺陷影响下硅材料的输出饱和阈值从小到大排序为:弗兰克尔缺陷 & 双空位缺陷、肖特基缺陷、本征硅。图 6(b)显示,按不同占位的自间隙原子影响下硅材料的输出饱和阈值从小到大排序为:双间隙原子缺陷、四面体间隙缺陷、六边形间隙缺陷、本征硅。在这几种缺陷处于

相同浓度的情况下,双间隙原子缺陷对于硅材料在 532 nm 这种带内激光作用下的吸收响应最强,故此时的饱和阈值最低,相比于本征态降低了 48.89%。

图 7 所示为 1319 nm 激光辐照下本征点缺陷对硅材料响应特性的影响。可以看出,本征点缺陷对于 1319 nm 带外激光和 532 nm 带内激光辐照下硅材料响应特性的影响有较大不同。当辐照波长为 1319 nm 时,本征硅几乎不吸收光子,很难产生响应输出。本征点缺陷的存在使得材料吸收边发生“红移”,同时明显增强了红外波段的光吸收,因此硅材料能够在此波长下产生较强的带外响应输出。图 7(a)显示双空位缺陷影响下的饱和阈值相对最小,为  $0.0086 \text{ W} \cdot \text{cm}^{-2}$ ;图 7(b)显示四面体间隙缺陷影响下的饱和阈值相对最小,为  $0.0015 \text{ W} \cdot \text{cm}^{-2}$ 。相同浓度的空位和自间隙缺陷相比,四面体间隙缺陷对于硅材料光电响应特性的影响最大,导致此时的输出饱和阈值在几种本征点缺陷的影响下为最低值。典型波长激光辐照下硅基光敏单元的饱和阈值如表 4 所示,其分析结果与前文一致。

## 4 结 论

针对空位和自间隙原子这两种硅单晶材料中固有的本征点缺陷,根据第一性原理建立了含有缺陷的硅

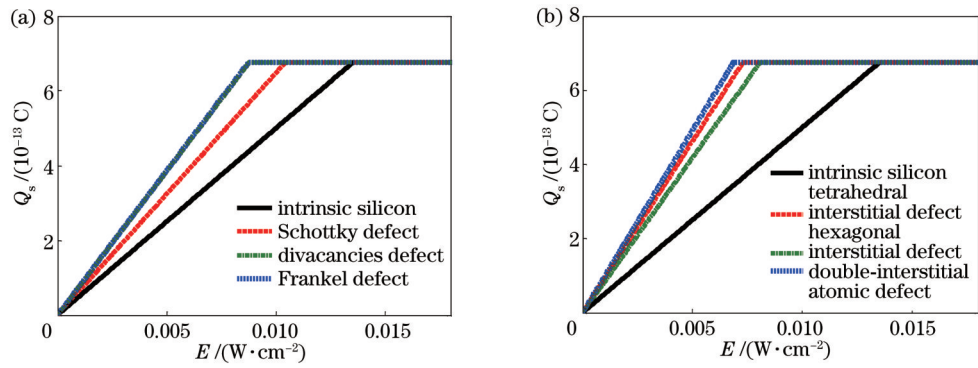


图 6 532 nm 激光辐照下本征点缺陷对硅材料响应特性的影响。(a)空位缺陷;(b)自间隙原子缺陷

Fig. 6 Effects of intrinsic point defects on the response characteristics of silicon materials under the irradiation of 532 nm laser.

(a) Vacancy defects; (b) self-interstitial atomic defects

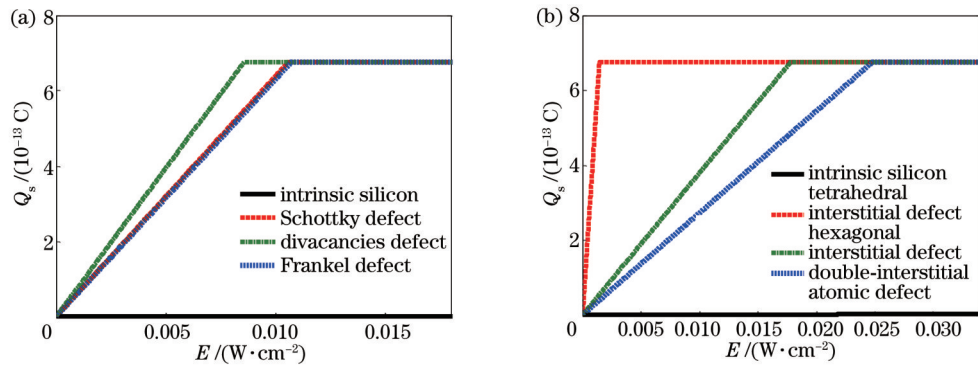


图 7 1319 nm 激光辐照下本征点缺陷对硅材料响应特性的影响。(a)空位缺陷;(b)自间隙原子缺陷

Fig. 7 Effects of intrinsic point defects on the response characteristics of silicon materials under the irradiation of 1319 nm laser.

(a) Vacancy defects; (b) self-interstitial atomic defects

表 4 本征点缺陷影响下硅基光敏单元的饱和阈值

Table 4 Saturation threshold of silicon-based photosensitive units affected by intrinsic point defects

Wavelength /nm	Saturation threshold $/( \text{W} \cdot \text{cm}^{-2} )$						
	Intrinsic silicon	Schottky defect	Divacancies defect	Frankel defect	Tetrahedral interstitial defect	Hexagonal interstitial defect	Double- interstitial atomic defect
532	0.0135	0.0104	0.0088	0.0087	0.0073	0.0081	0.0069
1319	6.8238	0.0106	0.0086	0.0107	0.0015	0.0178	0.0248

晶胞模型,分析了不同类型的空位缺陷和自间隙原子缺陷对硅材料能级结构的影响,具体计算了 532 nm 和 1319 nm 这两种典型激光辐照下硅材料的响应输出特性,比较了不同空位和自间隙原子缺陷对实际输出的影响。结果表明,空位缺陷和自间隙原子缺陷均会在禁带中引入缺陷能级,改变硅材料的能级结构,使得硅材料在可见光和红外波段都有明显的响应增强。对于 532 nm 带内激光,不同类型缺陷影响下硅基光敏单元的饱和阈值有不同程度的降低。对于理论上不会响应的 1319 nm 带外激光,相同浓度下四面体间隙缺陷对于硅材料的性质变化最为明显,即可以认为硅材料在 1319 nm 激光辐照下产生的带外响应主要是由硅中存在的四面体间隙缺陷导致的。此时,费米能级进入导带,材料带隙消失,吸收系数高达  $50391 \text{ cm}^{-1}$ ,折射率

相比于本征硅减小了 25.99%,从而导致量子效率增大为 0.2901,表明硅材料在该波长下能够产生较强响应,输出饱和阈值为  $0.0015 \text{ W} \cdot \text{cm}^{-2}$ 。

### 参 考 文 献

[1] Soref R A. Silicon-based optoelectronics[J]. Proceedings of the IEEE, 1993, 81(12): 1687-1706.  
 [2] 季渊, 许怡晴, 陈宝良, 等. 硅基微显示器发展现状与研究进展[J]. 激光与光电子学进展, 2022, 59(20): 2011007.  
 Ji Y, Xu Y Q, Chen B L, et al. Development and research progress of silicon-based microdisplays[J]. Laser & Optoelectronics Progress, 2022, 59(20): 2011007.  
 [3] 张璐, 柯少颖, 汪建元, 等. 硅基 IV 族材料外延生长及其发光和探测器件研究进展[J]. 中国科学: 物理学 力学 天文学, 2021, 51(3): 45-57.  
 Zhang L, Ke S Y, Wang J Y, et al. Research progress in the epitaxial growth of silicon-based group IV materials, and their

- light emitters and photodetectors[J]. *Scientia Sinica: Physica, Mechanica & Astronomica*, 2021, 51(3): 45-57.
- [4] 姚猛, 叶继飞, 李兰, 等. 皮秒激光辐照硅基光电二极管的饱和特性分析[J]. *激光与光电子学进展*, 2022, 59(13): 1304003. Yao M, Ye J F, Li L, et al. Analysis of saturation characteristics of silicon-based photodiodes irradiated by picosecond laser[J]. *Laser & Optoelectronics Progress*, 2022, 59(13): 1304003.
- [5] 杨柳, 蒋世磊, 孙国斌, 等. 等离子体增强金属-硅组合微结构近红外吸收[J]. *光学学报*, 2020, 40(21): 2124003. Yang L, Jiang S L, Sun G B, et al. Plasmonic enhanced near-infrared absorption of metal-silicon composite microstructure[J]. *Acta Optica Sinica*, 2020, 40(21): 2124003.
- [6] 张大勇, 赵剑衡, 王伟平, 等. 1.319  $\mu\text{m}$  连续 YAG 激光束对可见光面阵 CCD 系统的干扰研究[J]. *强激光与粒子束*, 2003, 15(11): 1050-1052. Zhang D Y, Zhao J H, Wang W P, et al. Study of disturbance to visible-light array CCD detectors irradiated by 1.319  $\mu\text{m}$  CW YAG laser[J]. *High Power Laser & Particle Beams*, 2003, 15(11): 1050-1052.
- [7] 张磊. 组合激光辐照半导体硅的耦合规律实验研究[D]. 长沙: 国防科学技术大学, 2008: 25-37. Zhang L. Experimental study on coupling law of semiconductor silicon irradiated by combined laser[D]. Changsha: National University of Defense Technology, 2008: 25-37.
- [8] 邱冬冬, 王睿, 程湘爱, 等. 连续激光对太阳能电池辐照效应的波段性研究[J]. *激光技术*, 2011, 35(5): 632-635, 683. Qiu D D, Wang R, Cheng X A, et al. Wave band effect of solar cells under irradiation of CW laser[J]. *Laser Technology*, 2011, 35(5): 632-635, 683.
- [9] Tang M J, Colombo L, Zhu J, et al. Intrinsic point defects in crystalline silicon: tight-binding molecular dynamics studies of self-diffusion, interstitial-vacancy recombination, and formation volumes[J]. *Physical Review B*, 1997, 55(21): 14279-14289.
- [10] Falster R, Voronkov V V, Quast F. On the properties of the intrinsic point defects in silicon: a perspective from crystal growth and wafer processing[J]. *Physica Status Solidi (b)*, 2000, 222(1): 219-244.
- [11] 刘彬. 本征缺陷和杂质对硅微纳结构机械性能的影响研究[D]. 长沙: 国防科学技术大学, 2016: 90-96. Liu B. Influence of intrinsic defects and impurities on mechanical properties of silicon micro-nano structures[D]. Changsha: National University of Defense Technology, 2016: 90-96.
- [12] Pei M, Wang W, Pan B C, et al. Calculation of defects in silicon by a new tight-binding model[J]. *Chinese Physics Letters*, 2000, 17(3): 215-217.
- [13] Dannefaer S, Avalos V, Andersen O. Grown-in vacancy-type defects in poly- and single crystalline silicon investigated by positron annihilation[J]. *The European Physical Journal Applied Physics*, 2007, 37(2): 213-218.
- [14] Lee Y J, Lee S, Hwang G S. Effects of vacancy defects on thermal conductivity in crystalline silicon: a nonequilibrium molecular dynamics study[J]. *Physical Review B*, 2011, 83(12): 125202.
- [15] 卜琼琼, 王堯, 靳映霞, 等. 自填隙原子对 Si 晶体性能影响的研究[J]. *红外技术*, 2012, 34(10): 598-601. Bu Q Q, Wang C, Jin Y X, et al. First-principles study influence of self-ion interstitial on properties of silicon crystal[J]. *Infrared Technology*, 2012, 34(10): 598-601.
- [16] 毛亦尘, 熊扬恒, 岳亚楠. 硅晶体热导率及点缺陷散射影响的分子动力学模拟[J]. *哈尔滨工业大学学报*, 2019, 51(7): 112-120. Mao Y C, Xiong Y H, Yue Y N. Thermal conductivity of silicon crystal and effects of point defect scatter by molecular dynamics[J]. *Journal of Harbin Institute of Technology*, 2019, 51(7): 112-120.
- [17] Clark S J, Segall M D, Pickard C J, et al. First principles methods using CASTEP[J]. *Zeitschrift Für Kristallographie-Crystalline Materials*, 2005, 220(5/6): 567-570.
- [18] Perdew J P, Burke K, Ernzerhof M. Generalized gradient approximation made simple[J]. *Physical Review Letters*, 1996, 77(18): 3865-3868.
- [19] Vanderbilt D. Soft self-consistent pseudopotentials in a generalized eigenvalue formalism[J]. *Physical Review B*, 1990, 41(11): 7892-7895.
- [20] 陈弘达. 微电子与光电子集成技术[M]. 北京: 电子工业出版社, 2008: 91-92. Chen H D. Microelectronic and optoelectronic[M]. Beijing: Publishing House of Electronics Industry, 2008: 91-92.
- [21] Xu J, Zhao S H, Hou R, et al. Laser-jamming analysis of combined fiber lasers to imaging CCD[J]. *Optics and Lasers in Engineering*, 2009, 47(7/8): 800-806.
- [22] 曾雄文, 陆启生, 赵伊君, 等. CCD 的光电特性研究[J]. *强激光与粒子束*, 1999, 11(1): 47-51. Zeng X W, Lu Q S, Zhao Y J, et al. The photoelectric characteristic research of CCD[J]. *High Power Laser & Particle Beams*, 1999, 11(1): 47-51.

## Effects of Intrinsic Point Defects on Response Characteristics of Silicon

Lü Tong, Zhang Rongzhu\*

*College of Electronics and Information Engineering, Sichuan University, Chengdu 610065, Sichuan, China*

### Abstract

**Objective** Silicon materials are widely used in the field of photoelectric detection because of their excellent optoelectronic properties. Theoretically, the long wave response limit of intrinsic silicon is about 1100 nm. However, it is found in experiments that silicon-based devices will also produce out-of-band response output under the irradiation of 1319 nm laser, which indicates that the photoelectric response characteristics of silicon materials deviate from the theoretical situation, which will cause significant interference to high-precision detection. The out-of-band responses of silicon-based devices indicate that the energy band structure of silicon materials has changed. Since intrinsic defects can change the energy levels of silicon materials, it is necessary to study the effects of intrinsic point defects in different states on the

photoelectric response characteristics of silicon materials. The theoretical analysis results can provide a reference for the subsequent application and development of silicon-based optoelectronic devices in the field of high-precision detection.

**Methods** The intrinsic point defects in single crystal silicon can change the band structures of silicon materials, thereby affecting the quality of materials and the performance of devices. Therefore, according to the intrinsic point defects of vacancies and self-interstitial atoms in single crystal silicon, cell models with defects in different states are established based on the first principles. The influence of intrinsic point defects on the band structure of silicon materials and the change in the optical properties of silicon materials under the influence of defects are analyzed. On this basis, the response output characteristics of silicon materials with intrinsic point defects under the irradiation of 532 nm and 1319 nm are calculated.

**Results and Discussions** The vacancy defects and self-interstitial atomic defects in different states will introduce defect energy levels into the energy level distribution of silicon, leading to the decrease or even disappearance of the band gap of silicon materials. These intrinsic point defects make the density of states move towards the low-energy direction as a whole (Fig. 2) and mainly affect the value of the density of states near the Fermi level, indicating that the number of energy levels within the energy range near the Fermi level increases significantly. Among several typical point defect states, the out-of-band response of silicon is mainly due to the influence of the tetrahedral interstitial defect. Under the irradiation of 1319 nm, the intrinsic silicon hardly absorbs photons, but the tetrahedral interstitial defect makes the absorption coefficient of silicon material as high as  $50391 \text{ cm}^{-1}$  [Fig. 3(b)], and the quantum efficiency increases to 0.2901 [Fig. 5(b)]. Thus, the silicon material can produce a strong response output to the irradiation of 1319 nm laser, making the output saturation threshold of the silicon-based photosensitive unit the minimum in several defect states, which is  $0.0015 \text{ W}\cdot\text{cm}^{-2}$  [Fig. 7(b)].

**Conclusions** For the intrinsic point defects inherent in silicon materials like vacancies and self-interstitial atoms, cell models with defects in different states are established based on the first principles, and the effects of different types of vacancy defects and self-interstitial atomic defects on the energy level structure of silicon materials are analyzed. The response output characteristics of silicon materials under the irradiation of 532 nm and 1319 nm lasers are calculated in detail, and the effects of different vacancies and self-interstitial atomic defects on the actual output are compared. The results show that both vacancy defects and self-interstitial atomic defects will introduce defect levels into the band gap, thus changing the band structure of silicon materials and enhancing the response of silicon in visible and infrared bands. For the in-band laser of 532 nm, the saturation thresholds of the silicon-based photosensitive unit decrease to different degrees under the effects of different states of intrinsic point defects. For the out-of-band laser of 1319 nm which does not respond theoretically, the properties of silicon materials affected by the tetrahedral interstitial defect have the most obvious changes under the same concentration. In other words, the out-of-band response of silicon materials under the irradiation of 1319 nm laser is mainly caused by tetrahedral interstitial defects present in silicon. In this case, the Fermi energy level enters into the conduction band, making the band gap of silicon disappear. The absorption coefficient reaches  $50391 \text{ cm}^{-1}$ , and the refractive index decreases by 25.99% compared with the intrinsic silicon, making the quantum efficiency increase to 0.2901. Therefore, the silicon material can produce a strong response at this wavelength, resulting in a low output saturation threshold of  $0.0015 \text{ W}\cdot\text{cm}^{-2}$ . The theoretical analysis results can provide a reference for the subsequent application and development of silicon-based optoelectronic devices in the field of high-precision detection.

**Key words** materials; single-crystal silicon; photoelectric response; intrinsic point defects; first principle